The GalNAc-T Activation (GALA) Pathway: Drivers and Markers

Authors:
Joanne CHIA[1], Felicia TAY[1] and Frederic BARD[1,2]

Affiliations:
[1]Institute of Molecular and Cell Biology, 61 Biopolis Drive, Singapore 138673
[2]Department of Biochemistry, National University of Singapore, 21 Lower Kent Ridge Road, Singapore 119077

*Corresponding Author:
Email: fbard@imcb.a-star.edu.sg
Tel: +65 6586 9585
Fax: +65 6779 1117

Abstract

GALNTs are enzymes adding a GalNAc sugar to Ser and Thr residues in thousands of proteins in the secretory pathway, GALNTs are activated by trafficking from Golgi to ER, a process driven by the Src kinase. GALNTs relocation (aka GALA) drives high Tn levels, occurs frequently in liver tumors and is a key driver of tumor growth. Recently, Tabak and colleagues have contested that EGF stimulation can induce GALNTs relocation. Here, we show that, while moderate and sensitive to culture conditions, relocation induced by EGF is reproducible and detectable even in the images acquired by Tabak et al. EGF induced relocation is enhanced by expression of EGFR and strongly induced by depletion of ERK8. EGF also activates a novel, imaging-independent marker of GALA: the O-glycosylated form of ER resident protein PDIA4. In sum, we demonstrate that non-reproducibility was due to experimental errors and propose specific conditions to facilitate the study of the GALA pathway.

Introduction

Replicability is essential to the scientific progress and has been the subject of intense debate in recent years. In biomedical sciences, some authors have argued that a large fraction of scientific studies are unreproducible, calling into question the value of discoveries and initiating a fierce debate [1–3].

In a study posted on BioRxiv and later published, Tabak and colleagues questioned the replicability of findings we published in 2010 and the physiological relevance of the GALNTs Activation (GALA) pathway [4]. In this 2010 paper, we proposed that GALNTs enzymes are regulated through trafficking from the Golgi to the ER. We showed that this relocation is induced by the tyrosine kinase Src. We further proposed that stimulation of cells by growth factors such as EGF and PDGF is able to induce this relocation, consistent with one proposed mode of activation of Src. We showed evidences that the Arf1-COPI machinery responsible for Golgi to ER traffic is involved in this relocation. Furthermore, we showed evidences that GALNTs are active in the ER and that their activity is stimulated by the relocation, constituting a potent mechanism to control O-glycosylation, which we named the GALA pathway.

O-GalNAc glycosylation occurs on thousands of secreted and cell surface proteins and is essential for multicellular life [5–8]. O-glycans are built by the sequential addition of simple sugars. GALNTs initiate the sequence by adding an N-Acetylgalactosamine (GalNAc) to a Ser or Thr residue. The resulting structure is called the Tn antigen and recognised by lectins such as VVL and HPL. Tn is usually a biosynthetic intermediate that is modified by the addition of other sugars such as galactose by enzymes such as C1GALT [9]. Further extension can result in more complex O-glycans. Tn can also be sialylated by sialyl-transferases, producing Sialyl-Tn, which is not further modified [10].

The formation of Tn has received a lot of attention from glycobiologists because malignant tumors have long been reported to have dramatically increased levels of Tn [11,12]. The phenotype is shared by most types of solid malignant tumors and occuring at a frequency of 70-90%, begging the question of its underlying molecular mechanisms and role in tumor biology. A proposed mechanism is that cancer cells lose the activity of the Tn modifying enzymes, in particular through mutations or loss of expression of its X-linked dedicated chaperone called Cosmc [13]. The selective advantage of short O-glycans for tumor cells is not clear, albeit they could interact with endogenous lectins such as Galectins and promote signaling events [14]. Studies have documented that short O-glycans can induce oncogenic features [15]. However, mutations of Cosmc have been reported to be extremely rare [15,16] and recent studies have shown that loss of C1GALT activity slows tumor progression in a mammary tumor model [17].

In our 2010 paper, we proposed that an alternative mechanism can also drive high Tn: the relocation of GALNTs to the ER induces an accumulation of Tn in this organelle. Since the ER tends to mesh the whole cytoplasm, the result is an increase of total cellular staining [4]. Importantly, we have not detected other O-glycans in the ER so far, suggesting that GalNAc is not modified by C1GALT and other extension enzymes. As the ER is much larger than the Golgi with a high content of proteins, the abundance of substrate and the lack of Tn modification can yield large increases in Tn levels when relocation is marked.

In a subsequent study, using VVL staining fluorescence imaging and quantitative analysis on tissue microarrays, we evaluated Tn levels increase to be up to 10 to 15 folds in human breast cancer tissues [18]. We showed that the

pattern of Tn staining in these samples is consistent with an ER localisation [18]. Furthermore, expressing an ER-targeted form of GALNT2 or T1 in cell lines such as HeLa, MDA-MB-231 and HepG2, is sufficient to induce a 6 to 10 fold increase of total HPL staining intensity [4,18,19]. By contrast over-expressing the wild-type form of the enzyme has no or very limited effects on Tn. More recently, we have shown that relocation is also occurring in a majority of liver cancers in humans and in mice [19]. Expressing an ER-targeted GALNT1 in this tumor model strongly accelerates tumor growth. Together, these data suggest that GALNTs relocation to the ER has a selective advantage for tumor cells and is the main mechanism driving Tn increase in breast and liver tumors.

How is the relocation process controlled? An RNAi screening approach revealed that GALNTs relocation is under the control of a complex genetic network. Upon depletion of a number of genes, Tn cellular staining significantly increases. 12 different genes were validated [20]. In the case of the Ser/Thr kinase ERK8, Tn levels increase ranged from 6 to 15 folds depending on the experimental context. This study suggested that there might be many different mechanisms able to induce the relocation of GALNTs, which is highly dependent on the status of the intracellular signalling network. We found various evidences that pathways downstream of stimulation by growth factors such as EGF and PDGF are able to activate GALA [4,20]. However, stimulation by EGF and PDGF itself produce a relatively moderate relocation.

In their study, Tabak and colleagues used EGF and PDGF stimulation and GALNTs staining and reported that they could not observe a decrease GALNTs colocalisation with a Golgi marker or increase of colocalisation with an ER marker.

In the intervening months, we have gone back to our initial study and data sets, repeated several experiments and analysed raw data acquired by Herbomel et al. and shared during the process of publishing their study. We could confirm that EGF and PDGF stimulation does induce changes in the pattern of Tn and GALNT staining. We observed that these experiments are sensitive to culture conditions, in particular to FBS. We also found that the relatively moderate effect was present in the images acquired by Herbomel but could not be quantified by the analytical method they chose. Finally, we present different experiments and a new marker to facilitate the modeling and measurement of the GALA relocation process in vitro and in vivo.

Results

Batch differences in FBS affect growth factor response

While we were analysing the causes of discrepancy between our results and those of Tabak's group, we considered the possible influence of cell lines and culture conditions. HeLa cell lines are known to be highly variable [21]. However we had sent our cells to the NIH and it did not seem to improve their experiments.

We grow HeLa cells with 10% Fetal Bovine Serum (FBS) which contains various growth factors and cytokines. Before growth factor stimulation, the cells were washed twice with PBS before overnight starvation in serum-free media. Over the years, we observed that different batches of FBS can have an effect on basal levels of Tn. We compared how different batches of FBS might affect the experiment. With some batches of FBS, we were able to observe an increase of 1.5 to 2 fold in Tn levels after 6h of EGF stimulation and to a lower extent with PDGF treatment (Fig 1A, 1B). However, we were surprised to find that when grown with other FBS batches, the effect of EGF or PDGF was minimal to sometimes undetectable (Fig 1C). Thus, contrary to expectation, washing and overnight FBS starvation does not completely erase the effect of previous growth conditions and can lead to a lack of response to EGF or PDGF.

EGFR levels strongly affect GALA response to EGF stimulation

A long term effect of FBS batches could be the level of growth factor receptors expressed. To test the importance of the levels of EGFR, we transfected HeLa cells with EGFR, then stimulated them with EGF. Expressing the receptor led to increase in Tn levels of more than 6 fold on average (Fig 1D, 1E). The effect was relatively variable between cells, with up to 20 fold increase after 4h EGF stimulation in some cells (Fig 1E). Thus, EGF stimulation can clearly increase GALA levels and this is highly dependent on the levels of EGFR.

Imaging and analysis method significantly affect GALA quantification

The extent by which imaging modalities can affect results can easily be underestimated. Using high throughput automated imaging conditions, we observe a 1.5-2 fold increase in Tn levels at 6 hours (Fig 1A, 1B). However, by using high resolution images acquired at 40X objective, we could quantify up to 4-fold increase at 6-hour (Fig 1F, S1A).

As previously noted in our commentary of their study, Herbomel et al. used confocal imaging at high magnification with extensive sectioning (61 slices), which is likely resulting in bleaching of the ER signal. Furthermore, the analytical method chosen by Herbomel et al. was inadequate to quantify relocation: the Manders coefficient ("M2") used to quantify relocation was measuring extent of colocalization of a Golgi marker with HPL or GALNT [22]. However, for optimal sensitivity of the relocation, the opposite approach of quantifying colocalization of HPL with Golgi marker should be used (see also the description of quantification in M&M). Using our images, we could not quantify relocation using Herbomel's method ("M2") but could detect an effect using the alternative approach ("M1") (Fig 1G, S1B). The Journal of Cell Biology requested the raw images used in Herbomel study and shared them. We used these images to run a quantification and we could again detect an effect both for GALNT and HPL

(Fig 1H, 1I and S1C). We conclude that the lack of effect reported by Herbomel et al. is due at least in part to their imaging and image analysis methods.

Tn levels increase after EGF stimulation are due to GALNT1/2 activity

HPL and VVL stainings have been associated with structures alternative to Tn. A concern of Dr. Tabak during our exchange of emails was that we were using HPL or VVL staining instead of relying only on GALNTs. To verify that the increase in Tn levels was indeed due to an increase in GALNTs activity, we performed a double knock-down of GALNT1 and 2, the main GALNTs expressed in Hela cells [23]. Depleting them completely abrogated the increase in Tn induced by EGF (Fig 1J).

Direct visual assessment of GALNTs ER relocation by immunofluorescence requires a marked relocation

EGF stimulation effect on the intracellular distribution of GALNTs can be observed in optimal conditions of culture and imaging. However, we found that the total levels of Tn is a more reliable and sensitive approach. At high resolution, after EGF stimulation, HPL staining appears highly disperse with a pattern reminiscent of the ER, while GALNTs distribution still appears at the Golgi, while more fragmented (Fig 2A). We interpret this difference as a consequence of the high dispersion effect of relocation on GALNTs. The ER is a much larger organelle than the Golgi and is distributed over the whole cytoplasm, so the GALNT signal is highly diluted. Because Tn is a more abundant antigen and its levels increase after relocation, its staining can still be detected in the ER. To illustrate the differences between Tn and GALNT stainings, we compared the same stainings after ERK8 depletion in HeLa cells (Fig 2B). In these conditions, Tn staining could easily be detected and was fully relocated to the ER while GALNT1 staining almost disappeared from cells (Fig 2B). In sum, observing the relocation process by directly staining for GALNTs requires strongly induced GALA and sensitive imaging methods.

Depletion of ERK8, a downstream target of EGFR signaling, leads to acute GALA activation

Growth factor stimulation leads to displacement of ERK8 from Golgi membranes and RNAi induced depletion of ERK8 leads to a marked GALA [20]. We compared the effects of ERK8 depletion after three days with EGF stimulation for 6 hours using identical cells and imaging conditions (Fig 2A,2B, S2A). While EGF stimulation induced a 4 fold increase in Tn levels, ERK8 depletion led to a 34 fold increase (Fig S2A). However, the two phenomenons appear to be related as treatment ERK8 depleted cells with the EGFR inhibitor AG-1478 reduced Tn levels by at least 40% (Fig 2C, S2A). Levels of Tn in human cancer tissues vary considerably but can often reach 20 fold increase compared to normal surrounding tissue levels. While the quantification method arguably differ between tissue sections and cells in culture, it suggests that acute depletion of ERK8 is better able to reflect the situation observed in human tumors. To note, we have not been able to establish a cell line stably depleted of ERK8.

To ascertain how general is ERK8 negative regulation of GALA, we repeated the knockdown in two other cell lines. SKOV3 is a cell line originating from an ovarian cancer, with epithelial characteristics. ERK8 depletion led to an 8 fold increase in Tn levels in these cells (Fig 2D, 2E). By contrast, knockdown in HepG2, an hepatocellular carcinoma, did not induce significant GALA.

To explore the mechanism by which ERK8 depletion leads to GALNT relocation, we labeled ERK8 depleted cells with a phospho-tyrosine antibody, PY20 (Fig 2F). Phosphotyrosine staining increased at the Golgi level by about 3 fold. This is highly reminiscent of the effect of Src activation at the Golgi [24]. Furthermore, treating cells with the Src tyrosine kinase inhibitor PP2 significantly reduced Tn levels (Fig 2H, S2C). This data indicates that after three days of knockdown, the tyrosine kinase and phosphatase balance at the Golgi had been durably affected. Whether this increase correspond to an increase in Src activity or to another related kinase is not clear at present since the more specific Src inhibitor SKI-1 (CAS 179248-59-0) did not reduce ERK8 depletion induced GALA.

The ER resident protein PDIA4 is a reliable marker of GALA activation.

As discussed above, imaging to quantify the levels of GALNT relocation has certain technical limitation. We searched for an independent biochemical marker. In our 2010 paper, we showed that a reporter protein we called ER-MUC5-GFP, a fragment of the mucin MUC5, fused with a signal sequence, GFP and an ER retention signal is hyperglycosylated upon Src activation. While a sensitive system for ER localised GALNT activity, the obvious limitation of this reporter system is that it requires transfection into cells. We recently identified PDIA4 as a resident ER protein that gets hyperglycosylated in tumors that show increased levels of Tn [19].

Here, we compared the increase of PDIA4 glycosylation with that of MUC-PTS. We used HEK293 cells as they are more easily transfected. We found that EGF and PDGF stimulation led to an increase in glycosylation levels of PDIA4 between 4 to 6 fold (Fig 3A, 3B). This increase was comparable or higher than with the ER-MUC5-GFP reporter (Fig 3A, 3B).

In Hela cells stimulated with EGF, PDIA4 glycosylation increased nearly three fold and was stimulated by expression of exogenous EGFR (Fig 3C, 3D).

We next measured PDIA4 glycosylation upon ERK8 depletion in HeLa cells and, consistent with our previous observations, obtained a robust, 6-fold increase in levels (Fig 3E, 3F). The same marker, PDIA4 glycosylation, was used to analyse liver tumors from mice (Fig 3G; see [19] for a description of the cancer model). The levels of PDIA4 glycosylation in healthy liver were low and glycosylation increased as tumors progressed, from 2-11 fold at early stages to 18-24 fold at late stage of tumor development. These increases mirror the total levels of Tn staining. Thus PDIA4 glycosylation demonstrate a correlation between increased Tn levels at the histological level and GALNT activity on an ER resident protein.

Discussion

Factors influencing the reproducibility of biomedical studies are unfortunately varied and numerous. Even cell lines in culture are complex and variable systems with genetic drift and components poorly defined such as FBS. Some phenomenons are more sensitive to these variations than others. In this study, we have sought to understand why Herbomel and colleagues were not able to reproduce our findings published in 2010. While it is difficult to ascertain exactly the reasons, we have identified two potential sources of discrepancy. One is the batch of FBS used to grow cells, which can affect GALA response. Effects of FBS batch on signaling are well documented and unfortunately hard to control [25]. The second source is the imaging and image analysis methods. Using images shared by Herbomel et al. and adjusting the image analysis protocol, we were able to detect GALA effect both on GALNT1 and on Tn staining, even if the effect was not directly visible in their published images.

It is possible that part of the confusion also arose from the fact that GALA is not an on/off system, but rather a rheostat-type regulatory process. This is in contrast with other signaling events such as activation of ERK1/2, which tends to function rather as an on/off switch. In cells stimulated by growth factors, GALA activation tends to be moderate. It correlates with the levels of activation of tyrosine kinases as evaluated by phospho-tyrosine levels. Src (or related tyrosine kinases) activation after EGF stimulation tends to be weaker than ERK1/2 (see for instance [26]. It also varies between cell lines. For instance, HEK293T responded with marked increase in phospho-tyrosines as detected by PY20 antibody as well as increase in Tn levels and Tn modification of PDIA4. By comparison, HeLa response was weaker both at the PY20 and PDIA4 Tn levels. Part of the discrepancy between the two labs could derive from a weak activation of Src in Herbomel study. Since they did not document Src activation, we cannot conclude on this point.

An active form of Src strongly induce the GALNTs relocation process, an observation that could be reproduced by Tabak's group (e-mail communication). A complication here is that too strong or too long a Src activation can also lead to Golgi fragmentation, especially in HeLa and other epithelial derived cell lines, as previously reported [27]. This can potentially muddle the measurement of relocation. For unknown reasons, Src activation induces more limited fragmentation in fibroblasts cell lines such as WI-38 or mouse embryonic fibroblasts such as the SYF cell line. A very clear segregation of GALNTs from other enzymes is then clearly observable.

By comparison with the growth factor stimulation experiment, our data indicate that GALA is strongly activated in most human breast and liver tumors. Obviously, this is the relevant context in which to consider this pathway. Are growth factors relevant *in vivo*? This is not clear at this stage. High levels of EGFR expression and activity are known to be associated with many different tumors, including breast [28] and liver [29]; so this receptor could potentially drive relocation in the pathological context. Src activity is strongly activated with many malignant transformation, so this could be a frequent (but not exclusive) driver of GALA in tumors [30]. In fine, most tumors display much higher levels of Tn than normal tissues and we propose that it is due most of the time to significant GALA activation. This claim can be relatively easily assessed by biochemical analysis of the glycosylation status of the ER resident protein PDIA4.

In a world increasingly concerned with scientific reproducibility, it is equally important to recognize the challenges when attempting reproduction[31]. The complexity of biological systems make a full control of experimental

parameters difficult while modern cell biology techniques can be challenging to master. In our own group, genome editing by CAS9-CRISPR was not ‘reproducible’ for months. Hopefully, the clarifications provided in this study will help other researchers who wish to study the GALA pathway address its significance in tumor progression.

Materials and methods

Cell culture

Hela cells were obtained from ATCC. Skov3 cells were a gift from E. Chapeau. Both Hela and Skov3 cells were grown in DMEM supplemented with 10% fetal bovine serum (FBS). HEK293T cells were a gift from W. Hong (IMCB, Singapore) and were grown in DMEM supplemented with 15% FBS. All cells were grown at 37°C in a 10% CO_2 incubator.

Reagents used in study

Recombinant human epidermal growth factor EGF (#SRP3027) was purchased from Sigma aldrich. PDGF-BB Recombinant Human Protein (#PHG0046), *Helix pomatia* Lectin A (HPL) conjugated with 647-nm fluorophore (#L32454) and anti-GFP (#A11122) were purchased from Thermo Fisher Scientific. Anti-Giantin (#ab24586), anti-actin (#ab8227), anti PDIA4 (#ab155800) antibodies were purchased from Abcam. Biotinylated Vicia Villosa Lectin (VVL; #B-1235) and agarose bound VVL (#AL-1233) were purchased from Vector Laboratories, Inc. Anti-phosphotyrosine clone PY20 (#05-947) and anti-phosphotyrosine clone 4G10 (#05-321) were purchased from Merck Millipore. Fetal bovine serum (FBS1; Gibco #10500-064 and FBS2 Gibco #16140-071) were purchased from Thermo Fisher Scientific.

Mouse anti-GALNT1 antibody in hybridoma supernatant was a gift from H. Clausen (University of Copenhagen, Denmark). GFP tagged epidermal growth factor receptor (EGFR) was a gift from W. Hong. siRNAs were purchased from Dharmacon, Inc.

EGFR inhibitor AG-1478 (#S2728) was purchased from Selleckchem. Src family kinase inhibitor PP2 (#529573) was purchased from Merck Millipore.

Cell transfection, growth factor stimulation and drug treatments

Plasmid transfection in Hela cells and HEK293T cells were performed with Fugene HD (Promega) and Lipofectamine 3000 (Thermo Fisher Scientific) respectively. Cells were transfected for at least 24 hours before further manipulations. siRNA transfection was described in detail in [32]. Briefly, 5µl of 500nM siRNA was mixed with 0.4µl of Hiperfect (Qiagen, #301705) and 14.6µl of Optimem (per well) for 20 min complexation, followed by the addition of 8000 cells to the transfection mix.

For growth factor stimulation, cells were washed twice using Dulbecco's phosphate-buffered saline (D-PBS) before overnight serum starvation in serum-free DMEM. Human recombinant EGF (100 ng/ml; Sigma-Aldrich) or mouse recombinant PDGF-bb (50 ng/ml;Invitrogen) were added for various durations before fixation with paraformaldehyde or lysed with RIPA lysis buffer.

For drug treatments, drugs were prepared by reconstituting in DMSO in concentrated stock solutions. The drugs or DMSO control were diluted in media containing 10% FBS and added to cells for 6 hours (AG-1478) or 24 hours (PP2) before fixation.

Immunofluorescence (IF) microscopy

For automated imaging, Hela cells were seeded in a 96-well clear and flat-bottomed black imaging plate (Falcon, #353219) and incubated overnight at 37°C and 10% CO_2 before growth factor stimulation or plasmid transfection. IF staining procedures was performed as reported in [4,33]. Cells were washed once with D-PBS before fixation with 4%-parafomaldehyde -4% sucrose in D-PBS for 10 minutes. Cells were washed once with D-PBS and permeabilised with 0.2% Triton-X for 10 minutes before the addition of primary antibody in blocking buffer 2% FBS in D-PBS. After primary antibody incubation, cells were washed with blocking buffer for 3 times and subsequently stained for 20 minutes with 2 μg/ml HPL, 5 μg/ml secondary Alexa Fluor–conjugated antibody and 1 μg/ml Hoechst (Invitrogen) in blocking buffer. Cells were then washed for 3 times with D-PBS before imaging. During automated image acquisition, nine sites per well were acquired sequentially with a 20X magnification Plan Fluor on automated imaging system (ImageXpress MICRO [IXM], Molecular devices, LLC). At least three replicate wells for each condition was performed.

For high resolution microscopy, cells were seeded onto glass coverslips in 24-well dishes (Nunc, Denmark). The procedures for IF staining were the same as described above. To observe phosphotyrosine staining, the cells were permeabilised with 0.2% Triton-X for 2 hour at room temperature and stained with anti-phosphotyrosine clone PY20 antibody diluted in 2% FBS in D-PBS overnight. Cells were mounted onto glass slides using FluorSave (Merck) and imaged with immersol oil using an inverted confocal microscope (Zeiss LSM700) at 40X, 60X or 100X magnification.

Quantification of Immunofluorescence (IF) Staining

Image analysis of HPL intensity of images acquired on IXM was performed using MetaXpress software (version 5.3.0.5). For each well, total HPL staining intensity and nuclei number was quantified using the 'Transfluor HT' application module in the software. Hundreds of cells from at least three wells per experiment were quantified. Two experimental replicates was performed.

For ImageJ analysis of HPL intensities, images were exported as 16-bit TIFF files. A fixed threshold for a mask on the HPL channel was set and the total intensity per image was calculated based on the total pixel count multiplied by the intensity per pixel. The HPL intensity per cell was then obtained by normalising the total image intensity with the nuclei count.

For analysis of Mander's coefficient, the images were analysed with ImageJ plugin (Just Another Colocalization Plugin, JACOP). A fixed threshold to distinguish from background signal was set on both HPL and Golgi channels for all images and the corresponding fraction of HPL coincident with Golgi channel ("M1") and fraction of Golgi coincident with HPL ("M2") was then used to quantify the colocalization between the markers.

Tabak's group provided one representative image stack from each experimental condition in .nd2 file format. Each image stack comprise of a z-stack of 61 images for each channel. Each image contains 3-4 cells acquired at 60x magnification. To analyse images provided by Tabak's group, an ImageJ plugin (Nikon ND2 Reader) was used to export z-stacks of each channel in .avi format. The Mander's coefficient was analysed with JACOP using the z-

stacks from different channels whereby a fixed threshold was set for each of the two channels in the set of images within the same experiment.

Image analysis of phosphotyrosine levels at the Golgi were quantified using the 'Translocation-enhanced' application module in the software whereby the intensity of PY20 staining within the Golgi area (demarcated by Giantin staining) per cell was quantified.

Lectin immunoprecipitation (IP)

Cells were washed twice with ice-cold D-PBS before lysis with RIPA lysis buffer containing protease and phosphatase inhibitor (Roche). The protein concentrations of clarified cell/ tissue lysates were measured using the Bradford reagent (Bio-Rad) and normalised across samples. At least 1mg of total lysate was incubated with VVL-conjugated beads for overnight at 4°C. The beads were washed at least three times with RIPA lysis buffer, before the precipitated proteins were eluted in 2x LDS sample buffer with 50mM DTT by boiling at 95°C for 10 minutes. The samples were resolvedby SDS-PAGE electrophoresis using bis-tris NuPage gels as per the manufacturer's instructions (Thermo Fisher Scientific) and transferred to nitorcellulose membranes. Membranes were then blocked using 3% BSA dissolved in Tris buffered saline with tween (TBST: 50 mM Tris [pH 8.0, 4°C], 150 mM NaCl, and 0.1% Tween 20) for 2 hours at room temperature before incubation with lectin or antibodies overnight. Membranes were washed at least three times with TBST before incubation with secondary HRP-conjugated antibodies (GE Healthcare). Membranes were further washed at least three with TBST before ECL (GE Healthcare) exposure.

Legends

Fig 1. FBS type, growth factor receptor levels and analysis methods affect interpretation of GALA activation by growth factor stimulation.

(A) *Helix pomatia* lectin (HPL) staining of Hela cells grown in FBS1 over time of EGF treatment (100 ng/ml). Images were acquired on ImageXpress Micro (IXM) at 20X magnification (air). Scale bar: 30 μm. HPL staining intensity of cells grown in (B) FBS1 and (C) FBS2 over time with 100 ng/ml EGF or 50 ng/ml PDGF stimulation. HPL intensity was analysed using the 'Transfluor HT' module of MetaXpress software (Molecular Devices) using the method described in [33]. Statistical significance (p) measured by two-tailed paired t test. *, $p < 0.05$ and **, $p < 0.01$ relative to mean HPL staining in unstimulated serum starved cells (0 h). NS, not significant. (D) Images of cells (60X magnification) transfected with EGFR-GFP stimulated with 100 ng/ml EGF for 4 hours. Scale bar: 10 μm. (E) Quantification of HPL intensity per cell that were untransfected (blue bars) or transfected with EGFR-GFP (green bars). At least 30 cells were quantified for each condition. Statistical significance (p) measured by two-tailed paired t test. *, $p < 0.05$ and ***, $p < 0.001$ relative to mean HPL staining in unstimulated cells (0 h). NS, not significant. (F) Quantification of HPL intensity on images acquired on 20X air lens (see images in (A)) and 40X lens under immersol oil (see images in Fig S1A) using ImageJ software. More than 100 cells were quantified for each condition. Statistical significance (p) measured by two-tailed paired t test. ***, $p < 0.001$ relative to mean HPL staining in corresponding unstimulated cells (0h). (G) Mander's coefficient to quantify the level of colocalization between HPL and Golgi marker MannII-GFP over time of EGF stimulation in Hela cells from Bard lab (see images in Fig S1B). M1 represents the fraction of HPL staining overlapping the Golgi and M2 represents the fraction of Golgi overlapping HPL staining. Values were normalised with respect to unstimulated control cells (0 h). Hundreds of cells were quantified. Statistical significance (p) measured by two-tailed paired t test. **, $p < 0.001$ relative to unstimulated cells (0 h). (H) Quantification of Mander's coefficient of HPL and Golgi marker TGN in representative images provided by Tabak's group. Each image provided contains 3 to 4 cells acquired at 60X magnification. Hela cells were stimulated with EGF and PDGF for 4 hours and 3 hours respectively. M1 represents the fraction of HPL staining overlapping the Golgi and M2 represents the fraction of Golgi overlapping HPL staining. Only M2 was presented in Herbomel et al. (I) Quantification of Mander's coefficient of GALNT1 and Golgi marker TGN in representative images provided by Tabak's group. (J) Quantification of HPL intensity of GALNT1 and GALNT2 siRNA knockdown cells ("siGALNT1+T2") and control cells treated with non-targeting siRNA ("siNT5") over time of EGF stimulation. Statistical significance (p) measured by two-tailed paired t test.*, $p < 0.05$, **, $p<0.01$ and ***, $p < 0.001$ relative to unstimulated cells (0h). NS, not significant.

Fig 2. ERK8 depletion induces acute GALA activation and occurs through EGFR pathway

Representative images of Hela cells stimulated with (A) 100 ng/ml EGF for 6 hours (B) ERK8 knockdown ("siERK8") and stained with HPL, GALNT1 and Golgi marker Giantin staining. Images were acquired at 100x magnification under immersol oil. Scale bar: 10 μm. (C) HPL staining intensity of ERK8 depleted Hela cells ("siERK8") treated with 10 μM EGFR inihibitor AG-1478 or DMSO control. "siNT" refers to non-targeting siRNA

treated cells. Statistical significance (p) measured by two-tailed paired t test. **p<0.01 relative to siERK8-DMSO control cells. (see images in Fig S2A) (D) HPL staining of Skov3 cells treated with non-targeting siRNA ("siNT") or ERK8 siRNA ("siERK8"). The Golgi is demarcated by MannII-GFP. Scale bar: 30 μm. (E) Quantification of HPL intensity of Skov3 cells in (D) using the 'Transfluor HT' module of MetaXpress software (Molecular Devices). (F) Phosphotyrosine staining (pY20) of Hela cells treated with non-targeting siRNA ("siNT") or ERK8 siRNA ("siERK8"). Images taken under 100X magnification under immersol oil. Scale bar: 10 μm. (G) Quantification of pY20 staining intensity in the Golgi region of non-targeting siRNA ("siNT") or ERK8 siRNA ("siERK8") treated cells using the 'Translocation-enhanced' module on MetaXpress. Images (20X magnification) were acquired on IXM. Statistical significance (p) measured by two-tailed paired t test.***, $p < 0.001$ relative to siNT cells. (H) Quantification of HPL intensity of ERK8 depleted Hela cells ("siERK8") treated with 10 μM Src inhibitor PP2 or DMSO control for 24 hours (See images in S2B). Statistical significance (p) measured by two-tailed paired t test. ***, $p < 0.001$ relative to siERK8-DMSO control.

Fig 3. **O-glycosylation ER resident protein PDIA4 is a reliable marker of GALA activation.**

(A) Immunoblot analysis of VVL IP on HEK cells exogenously expressing the ER specific O-glycosylation reporter ("ER-MUC5-GFP"). Cells were stimulated with 100 ng/ml EGF or 50 ng/ml PDGF stimulation over various durations. (B) Quantification of the levels of total VVL staining (orange), Tn modified ER-MUC5 reporter (green) and Tn modified endogenous ER resident PDIA4 in (A). Values were normalised with respect to the unstimulated cells. (C) Immunoblot analysis of VVL IP on Hela cells expressing EGFR or GFP control that were stimulated with 100 ng/ml EGF over the indicated durations. (D) Quantification of the levels of Tn modified endogenous ER resident PDIA4 in EGFR or GFP expressing cells over time of EGF stimulation in (C). (E) Immunoblot analysis of the levels of Tn modified PDIA4 in Hela cells treated with non-targeting siRNA ("siNT") or ERK8 siRNA ("siERK8"). (F) Quantification of the levels of Tn modified endogenous ER resident PDIA4 in (E). (G) Quantification of the levels of Tn modified endogenous ER resident PDIA4 in normal, NRas-G12V/shp53-injected mouse tumor samples at early (6 weeks post-injection; 6 wpi) stage and tumor samples from the late (24 wpi) stage [34].

References

1. Leek JT, Jager LR. Is Most Published Research Really False? Annual Reviews; 2017; doi:10.1146/annurev-statistics-060116-054104

2. Ioannidis JPA. How to make more published research true. PLoS Med. 2014;11: e1001747.

3. Ioannidis JPA. Contradicted and initially stronger effects in highly cited clinical research. JAMA. 2005;294: 218–228.

4. Gill DJ, Chia J, Senewiratne J, Bard F. Regulation of O-glycosylation through Golgi-to-ER relocation of initiation enzymes. J Cell Biol. 2010;189: 843–858.

5. Moremen KW, Tiemeyer M, Nairn AV. Vertebrate protein glycosylation: diversity, synthesis and function. Nat Rev Mol Cell Biol. 2012;13: 448–462.

6. Tran DT, Ten Hagen KG. Mucin-type O-glycosylation during development. J Biol Chem. 2013;288: 6921–6929.

7. Tian E, Ten Hagen KG. Recent insights into the biological roles of mucin-type O-glycosylation. Glycoconj J. 2009;26: 325–334.

8. Tarp MA, Clausen H. Mucin-type O-glycosylation and its potential use in drug and vaccine development. Biochim Biophys Acta. 2008;1780: 546–563.

9. Ju T, Brewer K, D'Souza A, Cummings RD, Canfield WM. Cloning and Expression of Human Core 1 β1,3-Galactosyltransferase. J Biol Chem. 2002;277: 178–186.

10. Munkley J. The Role of Sialyl-Tn in Cancer. Int J Mol Sci. 2016;17: 275.

11. Springer GF. T and Tn, general carcinoma autoantigens. Science. 1984;224: 1198–1206.

12. Springer GF. Tn epitope (N-acetyl-d-galactosamineα -O -serine/threonine) density in primary breast carcinoma: A functional predictor of aggressiveness. Mol Immunol. 1989;26: 1–5.

13. Ju T, Aryal RP, Kudelka MR, Wang Y, Cummings RD. The Cosmc connection to the Tn antigen in cancer. Cancer Biomark. 2014;14: 63–81.

14. RodrÍguez E, Schetters STT, van Kooyk Y. The tumour glyco-code as a novel immune checkpoint for immunotherapy. Nat Rev Immunol. 2018; doi:10.1038/nri.2018.3

15. Radhakrishnan P, Dabelsteen S, Madsen FB, Francavilla C, Kopp KL, Steentoft C, et al. Immature truncated O-glycophenotype of cancer directly induces oncogenic features. Proc Natl Acad Sci U S A. 2014;111: E4066–75.

16. Yoo NJ, Kim MS, Lee SH. Absence of COSMC gene mutations in breast and colorectal carcinomas. APMIS. 2008;116: 154–155.

17. Song K, Herzog BH, Fu J, Sheng M, Bergstrom K, McDaniel JM, et al. Loss of Core 1-derived O-Glycans Decreases Breast Cancer Development in Mice. J Biol Chem. 2015;290: 20159–20166.

18. Gill DJ, Tham KM, Chia J, Wang SC, Steentoft C, Clausen H, et al. Initiation of GalNAc-type O-glycosylation in the endoplasmic reticulum promotes cancer cell invasiveness. Proc Natl Acad Sci U S A. 2013;110: E3152–61.

19. Nguyen AT, Chia J, Ros M, Hui KM, Saltel F, Bard F. Organelle Specific O-Glycosylation Drives MMP14 Activation, Tumor Growth, and Metastasis. Cancer Cell. 2017;32: 639–653.e6.

20. Chia J, Tham KM, Gill DJ, Bard-Chapeau EA, Bard FA. ERK8 is a negative regulator of O-GalNAc glycosylation and cell migration. Elife. 2014;3: e01828.

21. Frattini A, Fabbri M, Valli R, De Paoli E, Montalbano G, Gribaldo L, et al. High variability of genomic instability and gene expression profiling in different HeLa clones. Sci Rep. 2015;5: 15377.

22. Herbomel GG, Rojas RE, Tran DT, Ajinkya M, Beck L, Tabak LA. The GalNAc-T Activation Pathway (GALA) is not a general mechanism for regulating mucin-type O-glycosylation. PLoS One. 2017;12: e0179241.

23. Mandel U, Hassan H, Therkildsen MH, Rygaard J, Jakobsen MH, Juhl BR, et al. Expression of polypeptide GalNAc-transferases in stratified epithelia and squamous cell carcinomas: immunohistological evaluation using monoclonal antibodies to three members of the GalNAc-transferase family. Glycobiology. 1999;9: 43–52.

24. Bard F, Mazelin L, Péchoux-Longin C, Malhotra V, Jurdic P. Src regulates Golgi structure and KDEL receptor-dependent retrograde transport to the endoplasmic reticulum. J Biol Chem. 2003;278: 46601–46606.

25. van der Valk J, Bieback K, Buta C, Cochrane B, Dirks WG, Fu J, et al. Fetal Bovine Serum (FBS): Past - Present - Future. ALTEX. 2018;35: 99–118.

26. Parks EE, Ceresa BP. Cell surface epidermal growth factor receptors increase Src and c-Cbl activity and receptor ubiquitylation. J Biol Chem. 2014;289: 25537–25545.

27. Weller SG, Capitani M, Cao H, Micaroni M, Luini A, Sallese M, et al. Src kinase regulates the integrity and function of the Golgi apparatus via activation of dynamin 2. Proc Natl Acad Sci U S A. 2010;107: 5863–5868.

28. Masuda H, Zhang D, Bartholomeusz C, Doihara H, Hortobagyi GN, Ueno NT. Role of epidermal growth factor receptor in breast cancer. Breast Cancer Res Treat. 2012;136: 331–345.

29. Sasaki T, Hiroki K, Yamashita Y. The role of epidermal growth factor receptor in cancer metastasis and microenvironment. Biomed Res Int. 2013;2013: 546318.

30. Summy JM, Gallick GE. Treatment for advanced tumors: SRC reclaims center stage. Clin Cancer Res. 2006;12: 1398–1401.

31. Collins FS, Tabak LA. Policy: NIH plans to enhance reproducibility. Nature. 2014;505: 612–613.

32. Chia J, Goh G, Racine V, Ng S, Kumar P, Bard F. RNAi screening reveals a large signaling network controlling the Golgi apparatus in human cells. Mol Syst Biol. 2012;8: 629.

33. Chia J, Tham KM, Gill DJ, Bard-Chapeau EA, Bard FA. ERK8 is a negative regulator of O-GalNAc glycosylation and cell migration. Elife. 2014;3: e01828.

34. Nguyen AT, Chia J, Ros M, Hui KM, Saltel F, Bard F. Organelle Specific O-Glycosylation Drives MMP14 Activation, Tumor Growth, and Metastasis. Cancer Cell. 2017;32: 639–653.e6.

Supplemental figures

Fig S1. **Tn staining and GALNT2 analysis in growth factor stimulated cells.**

(A) HPL staining of cells stimulated with 100 ng/ml EGF over 6 hours or depleted with ERK8. Images were acquired on 40X lens under immersol oil. Scale bar: 10 μm. (B) HPL staining of cells stimulated with EGF over the indicated duration. The Golgi is demarcated by MannII-GFP. Scale bar: 30 μm. (C) Quantification of Mander's coefficient of GALNT2 and Golgi marker TGN in representative images provided by Tabak's group.

Fig S2. **Tn staining intensity levels in growth factor stimulation compared to ERK8 depletion.** (A) Quantification of HPL intensity of ERK8 depleted cells (grey bars) using ImageJ analysis. ***, $p < 0.001$ relative to mean HPL staining in corresponding unstimulated cells (0h) or siNT cells. (B) HPL staining of ERK8 depleted Hela cells ("siERK8") treated with 10 μM EGFR inhibitor AG-1478 or DMSO control. Scale bar: 30 μm. (C) HPL staining of ERK8 depleted Hela cells ("siERK8") treated with 10 μM Src inhibitor PP2 or DMSO control for 24 hours.

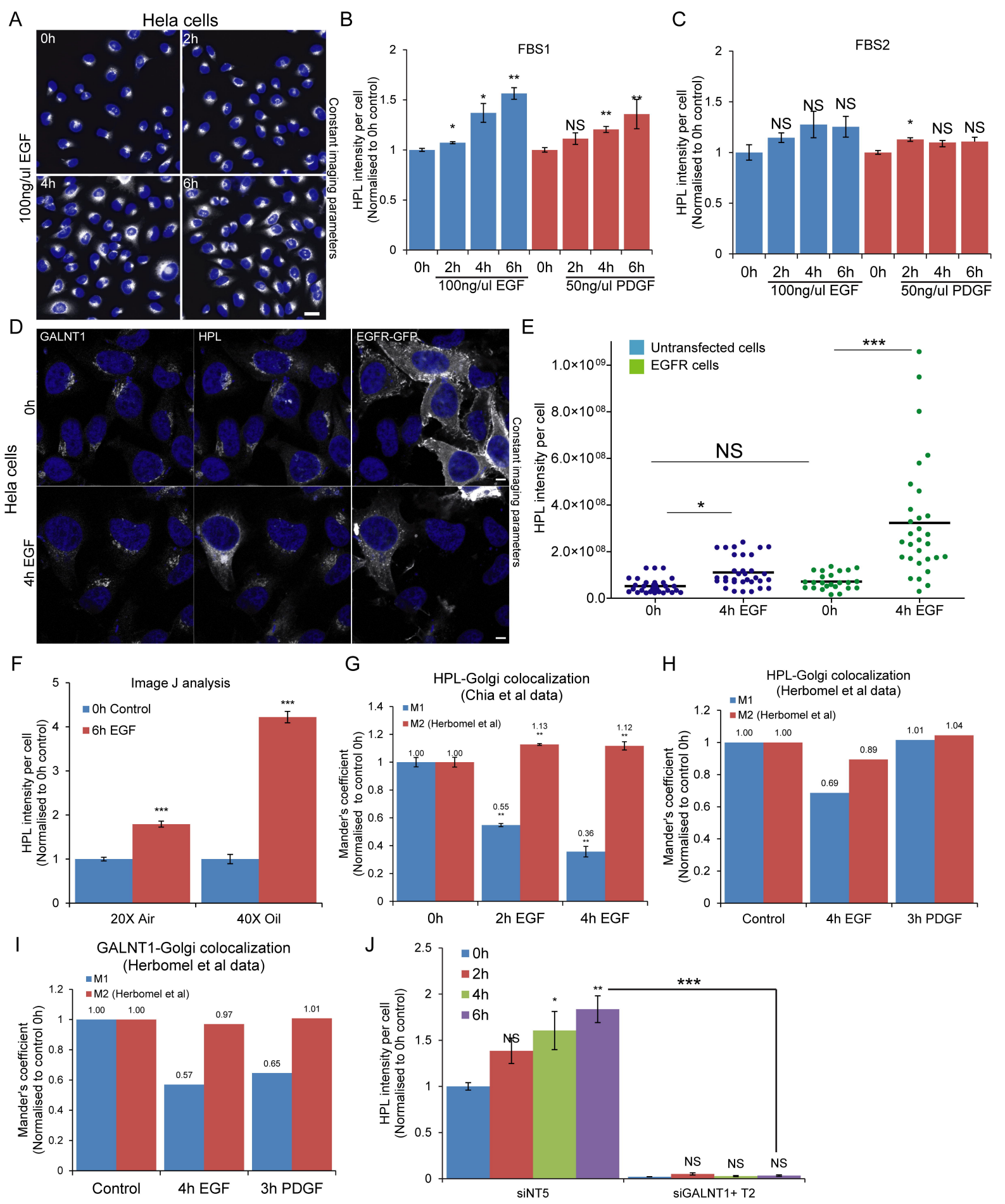
A
Hela cells
0h
2h
4h
6h
100ng/ul EGF
Constant imaging parameters
B
FBS1
HPL intensity per cell (Normalised to 0h control)
0h 2h 4h 6h 0h 2h 4h 6h
100ng/ul EGF
50ng/ul PDGF
C
FBS2
HPL intensity per cell (Normalised to 0h control)
0h 2h 4h 6h 0h 2h 4h 6h
100ng/ul EGF
50ng/ul PDGF
D
GALNT1
HPL
EGFR-GFP
Hela cells
0h
4h EGF
Constant imaging parameters
E
Untransfected cells
EGFR cells
HPL intensity per cell
0h
4h EGF
0h
4h EGF
F
Image J analysis
0h Control
6h EGF
HPL intensity per cell (Normalised to 0h control)
20X Air
40X Oil
G
HPL-Golgi colocalization (Chia et al data)
M1
M2 (Herbomel et al)
Mander's coefficient (Normalised to control 0h)
0h
2h EGF
4h EGF
H
HPL-Golgi colocalization (Herbomel et al data)
M1
M2 (Herbomel et al)
Mander's coefficient (Normalised to control 0h)
Control
4h EGF
3h PDGF
I
GALNT1-Golgi colocalization (Herbomel et al data)
M1
M2 (Herbomel et al)
Mander's coefficient (Normalised to control 0h)
Control
4h EGF
3h PDGF
J
0h
2h
4h
6h
HPL intensity per cell (Normalised to 0h control)
siNT5
siGALNT1+ T2

Figure 1

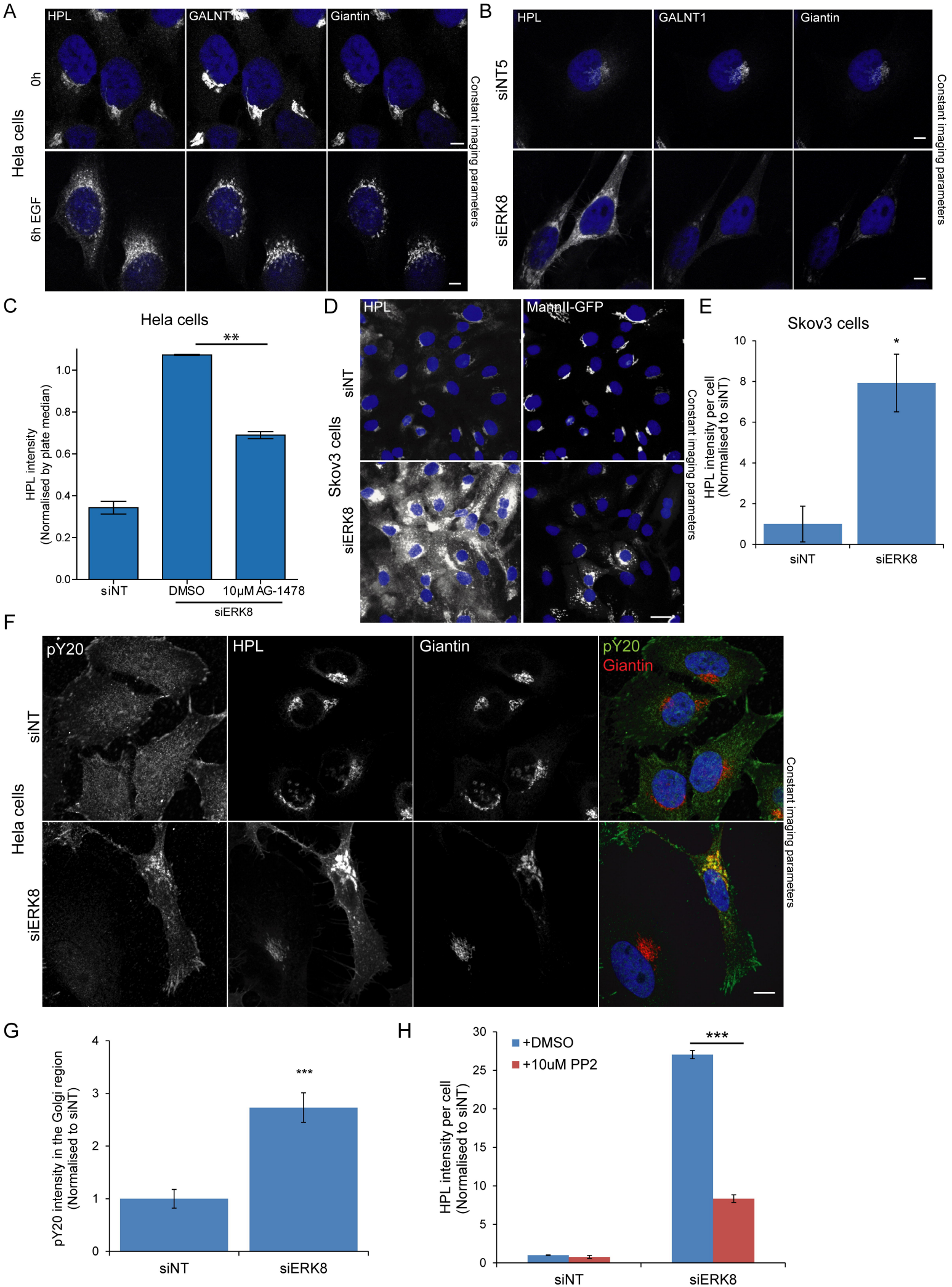
A
HPL
GALNT1
Giantin
Hela cells
0h
6h EGF
Constant imaging parameters
B
HPL
GALNT1
Giantin
siNT5
siERK8
Constant imaging parameters
C
Hela cells
**
HPL intensity
(Normalised by plate median)
1.0
0.8
0.6
0.4
0.2
0.0
siNT
DMSO
10μM AG-1478
siERK8
D
HPL
MannII-GFP
Skov3 cells
siNT
siERK8
Constant imaging parameters
E
Skov3 cells
*
HPL intensity per cell
(Normalised to siNT)
10
8
6
4
2
0
siNT
siERK8
F
pY20
HPL
Giantin
pY20
Giantin
Hela cells
siNT
siERK8
Constant imaging parameters
G
pY20 intensity in the Golgi region
(Normalised to siNT)
4
3
2
1
0
***
siNT
siERK8
H
+DMSO
+10uM PP2
***
HPL intensity per cell
(Normalised to siNT)
30
25
20
15
10
5
0
siNT
siERK8

Figure 2

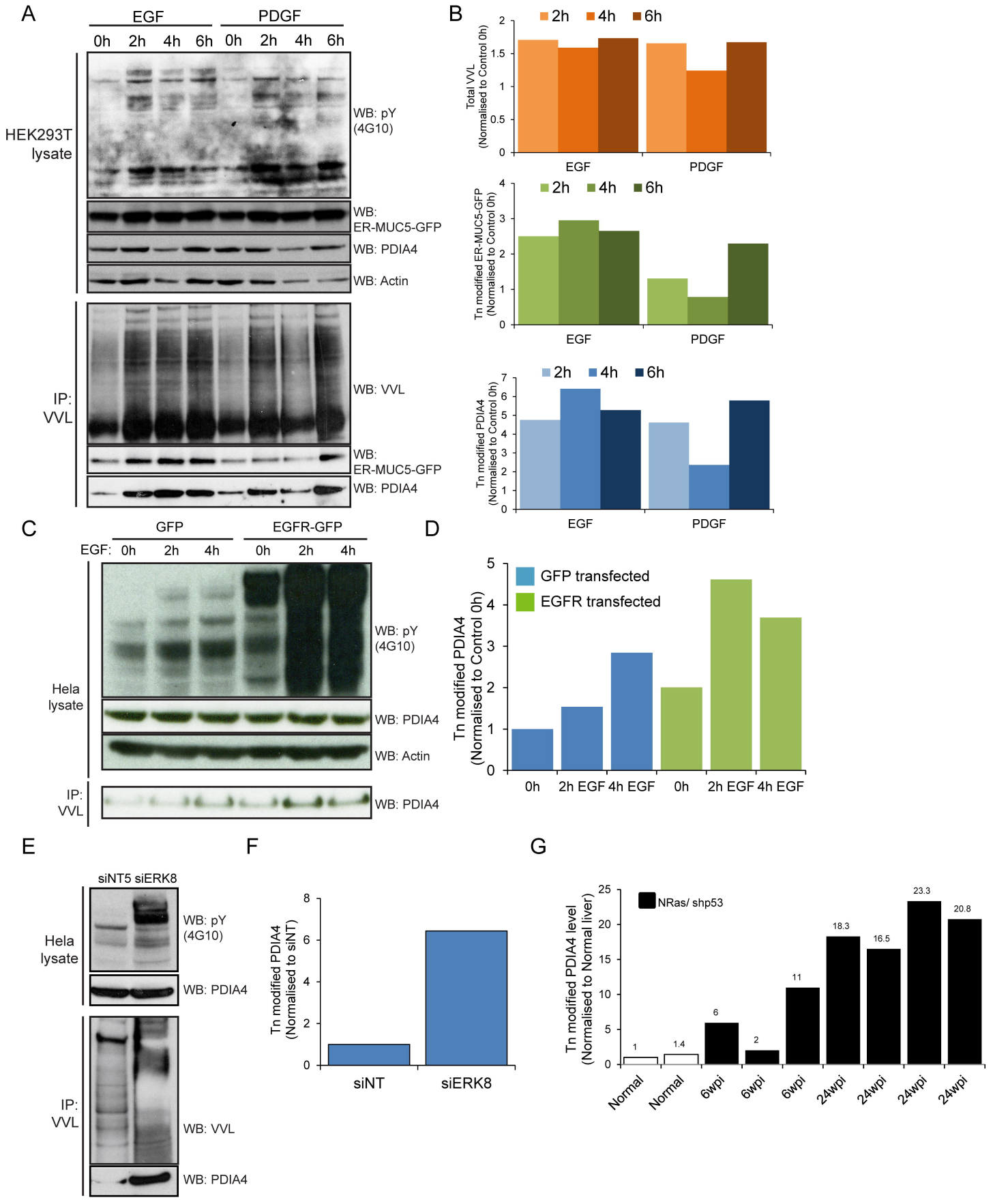
A
EGF
PDGF
0h 2h 4h 6h 0h 2h 4h 6h
HEK293T lysate
WB: pY (4G10)
WB: ER-MUC5-GFP
WB: PDIA4
WB: Actin
IP: VVL
WB: VVL
WB: ER-MUC5-GFP
WB: PDIA4
B
2h 4h 6h
Total VVL (Normalised to Control 0h)
Tn modified ER-MUC5-GFP (Normalised to Control 0h)
Tn modified PDIA4 (Normalised to Control 0h)
EGF
PDGF
C
GFP
EGFR-GFP
EGF: 0h 2h 4h 0h 2h 4h
Hela lysate
WB: pY (4G10)
WB: PDIA4
WB: Actin
IP: VVL
WB: PDIA4
D
GFP transfected
EGFR transfected
Tn modified PDIA4 (Normalised to Control 0h)
0h 2h EGF 4h EGF 0h 2h EGF 4h EGF
E
siNT5 siERK8
Hela lysate
WB: pY (4G10)
WB: PDIA4
IP: VVL
WB: VVL
WB: PDIA4
F
Tn modified PDIA4 (Normalised to siNT)
siNT
siERK8
G
NRas/ shp53
Tn modified PDIA4 level (Normalised to Normal liver)
1 1.4 6 2 11 18.3 16.5 23.3 20.8
Normal Normal 6wpi 6wpi 6wpi 24wpi 24wpi 24wpi 24wpi

Figure 3